Optica Applicata, Vol. LIV, No. 1, 2024
DOI: 10.37190/oa240103

Transverse electric guided modes in metal-LHM-ferrite slab waveguide structures

KHITAM Y. ELWASIFE*, MUSTAFA R. AL MASSRI, SOFYAN A. TAYA

Physics Department, Islamic University of Gaza, Gaza, Palestine

*Corresponding author: kelwasife@iugaza.edu.ps

TE guided modes at microwave frequencies in metal-left-handed material-ferrite waveguide structures are studied numerically. The effect of ferrite layer parameters on the dispersion properties of the waveguide structure is investigated in details. It is found that the modal index of the guided mode is negative as if the overall structure was left-handed material. A considerable effect of the gyromagnetic ferrite layer on the dispersion properties of the structure is observed. The power propagating in each layer is also evaluated.

Keywords: guided mode, left-handed material, metal, slab waveguide.

1. Introduction

Left-handed material (LHM) slab waveguide structures have received an increasing interest [1-13]. The study of electromagnetic wave properties guided by LHMs attracts much more attention. LHMs can be used in many applications such as the design of novel slab waveguide systems due to the peculiar properties of waves propagating in such structures. Waveguide structures containing LHMs were investigated for symmetric and asymmetric configurations [14-16]. RUPPIN studied the surface polaritons in a slab of LHM in the GHz frequency [3]. In 2008, WANG *et al.* studied the surface guided modes in slab waveguides with a LHM core and dielectric substrate and cladding [17]. Universal dispersion curves were plotted and analyzed. It was concluded that the guidance properties differ remarkably for different LHM constitutive parameters. Three normalized parameters were used to investigate the dispersion properties of different waveguide structures consisting of LHMs and nonlinear media [7,13,18]. Slab waveguide structures of LHM slab were found to support symmetric modes in asymmetric configuration [19]. The electric field profile of an asymmetric three-layer slab waveguide structure was studied in details [15]. A metal-clad waveguide with LHM core layer was also investigated [2,6]. A slab waveguide structure comprising lossy, dispersive, and anisotropic LHM layer was also studied [20-23]. The characteristics of propagating waves in a lossy LHM were investigated using finite-difference time-domain [24]. A novel wave absorber having the structure air/LHM/RHM/metal was proposed [25], where RHM stands for right-handed material of positive parameters. The properties of the proposed structure were numerically simulated and the results revealed that the absorbing bandwidth can be widened. A wave filter based on LHM was proposed and fabricated [26]. The length of the main part was only 1/20 compared to the working wavelength. Different waveguiding structures comprising LHM layer were studied for surface polariton condition [27]. The refection and transmission through a dielectric slab immersed in a medium of LHM was investigated [28]. A chiral material of negative index of refraction surrounded by dielectric media was proposed and analyzed [29]. The guidance characteristics of circular LHM rod waveguide including the dispersion properties and power confinement characteristics were studied [30]. Nonlinear waves guided by a LHM waveguide structure surrounded by a Kerr-like nonlinear dielectric was also investigated [31]. Due to the unusual properties of guided waves in LHMs, many potential applications were mentioned such as slab waveguide sensor [32-38] and bandpass filter [39]. KURSEEVA *et al.* have studied the propagation of transverse electric (TE) waves in a plane dielectric waveguide filled with nonlinear medium. The results of the above suggestion that the power nonlinearity and Kerr nonlinearity are qualitatively similar [40].

In this work, we present the dispersion relation and numerical results for TE guided waves propagating in metal-left-handed material-ferrite slab waveguide structure. LHM is considered a guiding layer bounded by a metal substrate and ferrite cladding. The power flow in each layer is also investigated. The effect of the ferrite layer parameters on the propagation characteristics is discussed in details.

2. Dispersion relation and power flow

Geometry of three layer slab waveguide structure is considered as shown in Fig. 1. It displays a waveguide structure which consists of left-handed material as a core layer in the region $0 \le z \le d$ surrounded by ferrite material as a cladding region of coordinate $z \ge d$ and metal substrate layer in the region $z < 0$. We assume stationary TE waves propagation along x-axis.

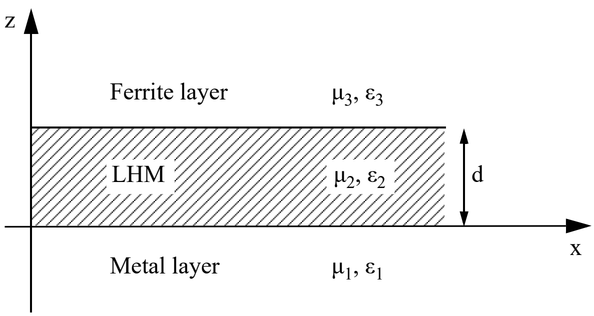

Fig. 1. Schematic geometry of left- handed material guiding film surrounded by ferrite layer as a cladding and metal layer as a substrate.

The metal layer has parameters ε_1 and μ_1, and the LHM has ε_2 and μ_2 of negative real part. The permeability tensor of the gyromagnetic ferrite cladding is [41]

$$\mu(\omega) = \begin{bmatrix} \mu_{xx} & 0 & i\mu_{xz} \\ 0 & \mu_{yy} & 0 \\ -i\mu_{xz} & 0 & -\mu_{xx} \end{bmatrix} \tag{1}$$

where $\mu_{xx} = \mu_B\left(1 + \dfrac{\omega_0\omega_m}{\omega_0^2 - \omega^2}\right)$, $\mu_{xz} = \mu_B\left(\dfrac{\omega\omega_m}{\omega_0^2 - \omega^2}\right)$, and $\mu_{yy} = \mu_B$ are the Polder tensor elements, with $\omega_0 = \gamma\mu_0 H_0$, $\omega_m = \gamma\mu_0 M_0$, and μ_B is the usual Polder tensor element; H_0 is the applied magnetic field, M_0 is the dc saturation magnetization and γ is the gyromagnetic ratio. The transverse electric and magnetic field components are

$$E = (0, E_y, 0)\exp\left[i(kx - \omega t)\right] \tag{2}$$

$$H = (H_x, 0, H_z)\exp\left[i(kx - \omega t)\right] \tag{3}$$

where ω is the angular frequency and k is the wave number in x-direction.

The E- and H-field components in three layer structure can by expressed as follows.

1) In the metal substrate the electric and magnetic fields are:

$$E_y^{(1)}(z) = A\exp(k_1 z) \tag{4}$$

$$H_x^{(1)}(z) = \frac{ik_1}{\omega\mu_1}A\exp(k_1 z) \tag{5}$$

$$H_z^{(1)}(z) = \frac{k}{i\omega\mu_1}A\exp(k_1 z) \tag{6}$$

where $k_1^2 = \beta^2 - (\omega^2/c^2)\mu_1\varepsilon_1$, and A is constant which can be determined from boundary conditions.

2) In the LHM core the electric and magnetic fields are:

$$E_y^{(2)}(z) = B\cos(k_2 z) + C\sin(k_2 z) \tag{7}$$

$$H_x^{(2)}(z) = \frac{i}{\omega\mu_z}\left[Ck_2\cos(k_2 z) - Bk_2\sin(k_2 z)\right] \tag{8}$$

$$H_z^{(2)}(z) = \frac{k}{i\omega\mu_z}\left[B\cos(k_2 z) + C\sin(k_2 z)\right] \tag{9}$$

where $k_2^2 = \beta^2 - (\omega^2/c^2)\mu_2\varepsilon_2$, B and C are constants to be obtained from the boundary condition.

3) In the ferrite cladding the electric and magnetic fields are:

$$E_y^{(3)}(z) = A\exp\left[-k_3(z-d)\right] \tag{10}$$

$$H_x^{(3)}(z) = \frac{-\mu_{xx}k_3 - \mu_{xz}k_3}{i\omega\mu_0\mu_{xx}\mu_v}E_y^{(3)}(z) \tag{11}$$

$$H_z^{(3)}(z) = \frac{-\mu_{xz}k_3 + \mu_{xx}k_3}{\omega\mu_0\mu_{xx}\mu_v}E_y^{(3)}(z) \tag{12}$$

where $k_3^2 = \beta^2 - (\omega^2/c^2)\mu_v\varepsilon_2$, and $\mu_v = (\mu_{xx}^2 - \mu_{xz}^2)/\mu_{xx}$ is the effective Voigt permeability. Applying the continuity of E_y and H_x across $z = 0$ and $z = d$, the following dispersion relation is obtained

$$\tan(k_2 d) = \frac{-\mu_{xx}k_3 + \mu_{xz}k + \mu_0\mu_{xx}\mu_v\dfrac{k_1}{\mu_1}}{\mu_0\mu_{xx}\mu_v\dfrac{k_2}{\mu_2} + \mu_{xx}k_3\dfrac{k_1\mu_2}{k_2\mu_1} + \mu_{xz}k\dfrac{k_1\mu_2}{k_2\mu_1}} \tag{13}$$

It is very important to evaluate the power flowing in each layer which is given by

$$P_{\text{total}} = \frac{\beta}{2\omega\mu}\mathrm{Re}\left(\int_{-\infty}^{\infty}|E_y|\,\mathrm{d}z\right) \tag{14}$$

from which

$$P_1 = \frac{\beta}{4\omega\mu_1 k_1} \tag{15}$$

$$P_2 = \frac{\beta}{4\omega\mu_2}\left[\frac{d}{2} + \frac{\sin(2k_2 d)}{4k_2} + \left(\frac{k_1\mu_2}{k_2\mu_1}\right)^2\frac{d}{2} - \left(\frac{k_1\mu_2}{k_2\mu_1}\right)^2\frac{\sin(2k_2 d)}{4k_2} + \left(\frac{k_1\mu_2}{k_2\mu_1}\right)^2\frac{\sin^2(2k_2 d)}{2k_2}\right] \tag{16}$$

$$P_3 = \frac{-\mu_{xz}k_3 + \mu_{xx}k}{\omega\mu_0\mu_{xx}\mu_v}\,\frac{1}{4\omega\mu_3 k_3}\left[\cos(k_2 d) + \frac{k_1\mu_2}{k_2\mu_1}\sin(k_2 d)\right]^2 \tag{17}$$

3. Numerical results and discussion

The dispersion relation was solved numerically to find the effective wave index k as a function of the angular frequency ω. The frequency range was taken from 17 to 18 GHz. The numerical calculations were carried out using the following parameters of the ferrite (YIG) cladding $\varepsilon_3 = 1$, $\gamma_f = 1.7 \times 10^{11}$ s^{-1}T^{-1} (subscript "f" refere to ferrite layer), $\mu_0 M = 0.175$ T, and $\omega_0 = \gamma_f \mu_0 H_0$. The thickness of the LHM guiding layer $d = 100$ μm, electric permittivity $\varepsilon_3 = \varepsilon_{3r} + \varepsilon_{3i}$, and magnetic permeability and $\mu_3 = \mu_{3r} + \mu_{3i}$. Where "i" and "r" represents imaginary and real part, respectively. The substrate is assumed to be metal with $\varepsilon_1 = -16 + 0.52i$ and $\mu_1 = 1$.

In Fig. 2, the effective wave index k is plotted *versus* the frequency for different values of γ_f. The effective wave index is smoothly decreasing with increasing frequen-

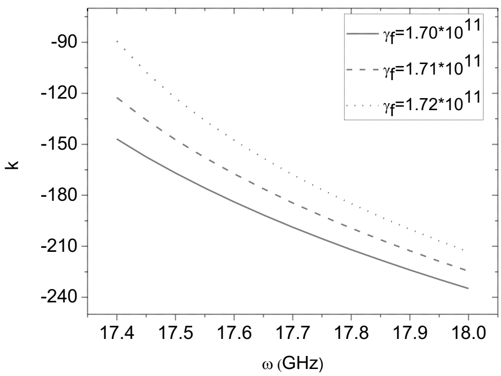

Fig. 2. The dispersion properties of the proposed structure for different values of γ_f, when $\varepsilon_1 = -16 + 0.52i$, $\mu_1 = 1$, $\varepsilon_2 = -5 + 0.01i$, $\mu_2 = -8 + 0.01i$, $d = 100$ μm, $\varepsilon_3 = 1$, $\mu_B = 1.25$, $\mu_0 M = 0.175$ T, $\mu_0 H_0 = 0.55$ T, $\omega_m = \gamma_f \mu_0 M$, and $\omega_{0f} = \gamma_f \mu_0 H_0$.

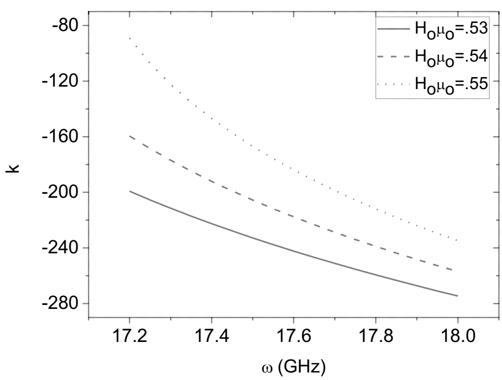

Fig. 3. The dispersion properties of the proposed structure for different value of $H_0\mu_0$ when $\varepsilon_1 = -16 + 0.52i$, $\mu_1 = 1$, $\varepsilon_2 = -5 + 0.01i$, $\mu_2 = -8 + 0.01i$, $d = 100$ μm, $\varepsilon_3 = 1$, $\gamma_f = 1.70 \times 10^{11}$ s^{-1}T^{-1}, $\mu_B = 1.25$, $\mu_0 M = 0.175$ T, $\omega_m = \gamma_f \mu_0 M$, and $\omega_{0f} = \gamma_f \mu_0 H_0$.

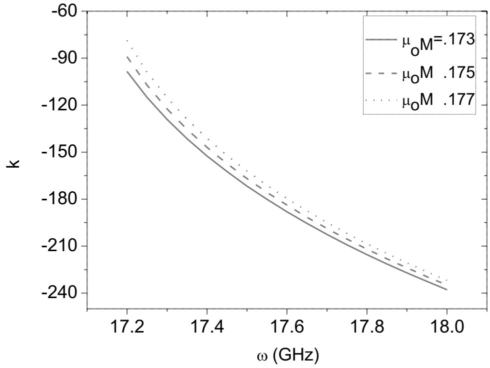

Fig. 4. The dispersion properties of the proposed structure for different values of $\mu_0 M$ when $\varepsilon_1 = -16 + 0.52i$, $\mu_1 = 1$, $\varepsilon_2 = -5 + 0.01i$, $\mu_2 = -8 + 0.01i$, $d = 100$ μm, $\varepsilon_3 = 1$, $\gamma_f = 1.70 \times 10^{11}$ $s^{-1}T^{-1}$, $\mu_B = 1.25$, $\mu_0 H_0 =$ $= 0.55$ T, $\omega_m = \gamma_f \mu_0 M$, and $\omega_{0f} = \gamma_f \mu_0 H_0$.

cy. The figure also reveals that for a given frequency, k can be enhanced by decreasing the value of gyromagnetic ratio γ_f. The range of frequencies over which the structure can support guided waves is strongly dependent on the static biasing magnetic field H_0 as can be seen from Fig. 3. This frequency range can be considerably enhanced by increasing the value of $\mu_0 H_0$. For $\mu_0 H_0 = 0.53$, 0.54, and 0.55, the structure can support guided waves in the frequency ranges 17.2 GHz $< \omega <$ 18 GHz. An important feature can be observed from the figure: the effective wave index of the structure is negative as if the overall structure is left-handed material. This means the reversal of the energy flow and that the group velocity and the phase velocity are in opposite directions. In Fig. 4, the effect of the DC magnetization of the magnetic insulator on the dispersion characteristics is studied. As can be seen, the dispersion curves shift towards higher frequencies with decreasing $\mu_0 M$. The magnetization of the magnetic insulator and the gyromagnetic ratio almost have the same effect on the dispersion characteristics of the proposed structure. The dispersion curves shift towards higher effective wave

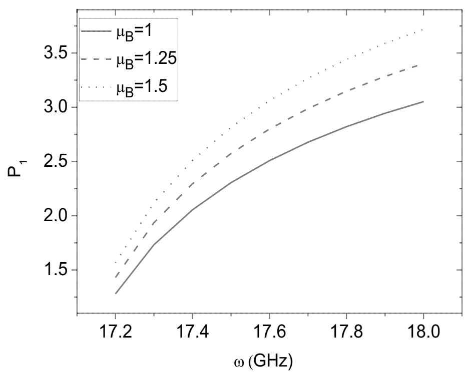

Fig. 5. Power flowing through metal layer when $\varepsilon_1 = -16 + 0.52i$, $\mu_1 = 1$, $\varepsilon_2 = -5 + 0.01i$, $\mu_2 = -8 + 0.01i$, $d = 100$ μm, $\varepsilon_3 = 1$, $\mu_B = 1.25$, $\mu_0 M = 0.175$ T, $\mu_0 H_0 = 0.55$ T, $\omega_m = \gamma_f \mu_0 M$, and $\omega_{0f} = \gamma_f \mu_0 H_0$.

index β with decreasing either $\mu_0 M$ or γ_f. The gyromagnetic ferrite layer parameters (H_0, $\mu_0 M$, γ_f) have a considerable effect on the dispersion properties of the structure. A slight change in the effective wave index is observed with increasing the ferrite layer parameters $\mu_0 M$.

The power flowing in each layer as a function of the propagating wave frequency is shown in Figs. 5, 6 and 7. The part of total power flowing in the cladding layer is a very important coefficient in the field of sensing using waveguide structure. The important of this part improves the sensitivity of the effective wave index to changes in the refractive index of the cladding. Figure 5 illustrates the power flowing through metal as a substrate layer when $\varepsilon_1 = -16 + 0.52i$ and $\mu_1 = 1$. As μ_B increases, the power curves move up showing an enhancement of the power. The power P_2 flowing in the LHM guiding layer is negative (Fig. 6.) which is an important feature that can be seen in these figure. This is one of the main differences between left- and right-handed ma-

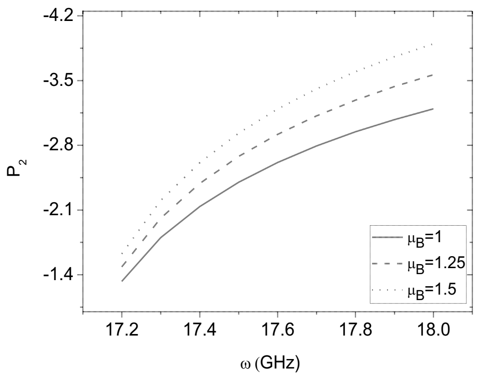

Fig. 6. Power flowing through LHM layer when $\varepsilon_1 = -16 + 0.52i$, $\mu_1 = 1$, $\varepsilon_2 = -5 + 0.01i$, $\mu_2 = -8 + 0.01i$, $d = 100$ μm, $\varepsilon_3 = 1$, $\mu_B = 1.25$, $\mu_0 M = 0.175$ T, $\mu_0 H_0 = 0.55$ T, $\omega_m = \gamma_f \mu_0 M$, and $\omega_{0f} = \gamma_f \mu_0 H_0$.

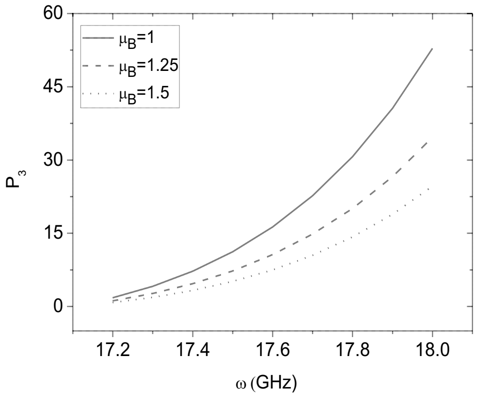

Fig. 7. Power flowing through ferrite cladding layer for different values of μ_B when $\varepsilon_1 = -16 + 0.52i$, $\mu_1 = 1$, $\varepsilon_2 = -5 + 0.01i$, $\mu_2 = -8 + 0.01i$, $d = 100$ μm, $\varepsilon_3 = 1$, $\mu_0 M = 0.175$ T, $\mu_0 H_0 = 0.55$ T, $\omega_m = \gamma_f \mu_0 M$, and $\omega_{0f} = \gamma_f \mu_0 H_0$.

terials. In RHM, the Poynting's vector **S** always forms a right-handed set with the vectors **E** and **H**. Accordingly, for RHMs **S** and the propagation vector **k** are in the same direction. However, this is not the case of LHMs in which **S** and **k** are in opposite directions. It is well known that the phase velocity and the propagation vector **k** are in the same direction for normal materials. Thus, it is clear that LHMs are substances with a so-called negative group velocity, which occurs in particular in anisotropic substances or when there is spatial dispersion. Figure 6 emphasizes the fact that in LHMs the phase velocity is opposite to the energy flow. The third layer is considered as the ferrite (YIG) cladding has the highest fractional of total power as shown in Fig. 7. This means that the proposed structure is a strong candidate for a non-communication application of slab waveguides such as optical sensing.

4. Conclusion

We have studied analytically the TE guided waves in a slab waveguide structure comprising a left-handed material film embeded between ferrite cover and metal substrate. The dispersion relation was derived and numerically investigated. It was found that the effective wave index is negative which means that the structure exhibits a LHM behavior. The range of frequencies over which the structure can support guided waves is strongly dependent on the gyromagnetic ferrite layer parameters. We noticed that the power flow is proportional to the angular frequency in metal, substrate and the ferrite cladding.

References

[1] ELWASIFE KH.Y., TAYA S.A., *Characteristics of symmetric left-handed material slab waveguide*, IOSR Journal of Applied Physics **8**(5), 2016: 91-98.

[2] HE Y., ZHANG X., YANG Y., LI C., *Guided modes in asymmetric metal-cladding left-handed material waveguides*, Chinese Optics Letters **9**(5), 2011: 052301.

[3] RUPPIN R., *Surface polaritons of a left-handed material slab*, Journal of Physics: Condensed Matter **13**(9),2001: 1811-1819. https://doi.org/10.1088/0953-8984/13/9/304

[4] VESELAGO V.G., *The electrodynamics of substances with simultaneously negative values of ε and μ*, Soviet Physics Uspekhi **10**(4), 1968: 509-514. https://doi.org/10.1070/PU1968v010n04ABEH003699

[5] TAYA S.A., *Theoretical investigation of slab waveguide sensor using anisotropic metamaterials*, Optica Applicata **45**(3), 2015: 405-417. https://doi.org/10.5277/oa150312

[6] TAYA S.A., ELWASIFE KH.Y., *Guided modes in a metal-clad waveguide comprising a left-handed material as a guiding layer*, International Journal of Research and Reviews in Applied Sciences (IJRRAS) **13**(1), 2012, 294-305.

[7] QADOURA I.M., TAYA S.A., ELWASIFE KH.Y., *Scaling rules for a slab waveguide structure comprising nonlinear and negative index materials*, International Journal of Microwave and Optical Technology (IJMOT) **7**(5), 2012: 349-357.

[8] SHALAEV V.M., *Optical negative-index metamaterials*, Nature Photonics **1**(1), 2007: 41-48. https://doi.org/10.1038/nphoton.2006.49

[9] KILDISHEV A.V., CAI W., CHETTIAR U.K., YUAN H.K., SARYCHEV A.K., DRACHEV V.P., SHALAEV V.M., *Negative refractive index in optics of metal-dielectric composites*, Journal of the Optical Society of America B **23**(3), 2006: 423-433. https://doi.org/10.1364/JOSAB.23.000423

[10] KAFESAKI M., KOSCHNY TH., ZHOU J., KATSARAKIS I., TSIAPA I., ECONOMOU E.N., SOUKOULIS C.M., *Electromagnetic behaviour of left-handed materials*, Physica B: Condensed Matter **394**(2), 2007: 148-154. https://doi.org/10.1016/j.physb.2006.12.044

[11] KULLAB H.M., QADOURA I.M.,TAYA S.A., *Slab waveguide sensor with left-handed material core layer for detection an adlayer thickness and index*, Journal of Nano- and Electronic Physics **7**(2), 2015: 02039.

[12] TAYA S.A., EL-FARRAM E.J., ABADLA M.M., *Symmetric multilayer slab waveguide structure with a negative index material: TM case*, Optik **123**(24), 2012: 2264-2268. https://doi.org/10.1016/j.ijleo.2011.11.016

[13] TAYA S.A., QADOURA I.M., *Guided modes in slab waveguides with negative index cladding and substrate*, Optik **124**(13), 2013: 1431-1436. https://doi.org/10.1016/j.ijleo.2012.03.057

[14] WU B.I., GRZEGORCZYK T.M., ZHANG Y., KONG J.A., *Guided modes with imaginary transverse wave number in a slab waveguide with negative permittivity and permeability*, Journal of Applied Physics **93**(11), 2003: 9386-9388. https://doi.org/10.1063/1.1570501

[15] TAYA S.A., ELWASIFE KH.Y., *Field profile of asymmetric slab waveguide structure with LHM layers*, Journal of Nano- and Electronic Physics **6**(2), 2014: 02007.

[16] HE Y., CAO Z., SHEN Q., *Guided optical modes in asymmetric left-handed waveguides*, Optics Communications **245**(1), 2005: 125-135. https://doi.org/10.1016/j.optcom.2004.09.067

[17] WANG Z.H., XIAO Z.Y., LUO W.Y., *Surface modes in left-handed material slab waveguides*, Journal of Optics A: Pure and Applied Optics **11**(1), 2009: 015101. https://doi.org/10.1088/1464-4258/11/1/015101

[18] TAYA S.A., KULLAB H.M., QADOURA I.M., *Dispersion properties of slab waveguides with double negative material guiding layer and nonlinear substrate*, Journal of the Optical Society of America B **30**(7), 2013: 2008-2013. https://doi.org/10.1364/JOSAB.30.002008

[19] MOKHTARI B., EDDEQAQI N.C., ATANGANA J., ESSAMA B.G., KOFANE T.C., *Impact of cladding permeability on guided modes in a negative-index slab waveguide*, International Journal of Emerging Technology and Advanced Engineering **4**(5), 2014: 719-726.

[20] TAYA S.A., *Slab waveguide with air core layer and anisotropic left-handed material claddings as a sensor*, Opto-Electronics Review **22**(4), 2014: 252-257. https://doi.org/10.2478/s11772-014-0201-3

[21] TAYA S.A., *P-polarized surface waves in a slab waveguide with left-handed material for sensing applications*, Journal of Magnetism and Magnetic Materials **377**, 2015: 281-285. https://doi.org/10.1016/j.jmmm.2014.10.126

[22] TAYA S.A., *Dispersion properties of lossy, dispersive, and anisotropic left-handed material slab waveguide*, Optik **126**(14), 2015: 1319-1323. https://doi.org/10.1016/j.ijleo.2015.04.013

[23] TAYA S.A., ELWASIFE KH.Y., KULLAB H.M., *Dispersion properties of anisotropic-metamaterial slab waveguide structure*, Optica Applicata **43**(4), 2013: 857-869. https://doi.org/10.5277/oa130420

[24] WU G., LIU S., ZHONG S., *Numerical analysis of propagation characteristics of electromagnetic wave in lossy left-handed material media*, Optik **125**(16), 2014: 4233-4237. https://doi.org/10.1016/j.ijleo.2014.04.018

[25] WANG Z., ZHANG Z., QIN S., WANG L., WANG X., *Theoretical study on wave-absorption properties of a structure with left- and right-handed materials*, Materials and Design **29**(9), 2008: 1777-1779. https://doi.org/10.1016/j.matdes.2008.03.015

[26] HUANG C., CHEN D., WEI W.J., JING X.M., CHEN X., LIU J.Q., ZHU J., WEI Z.Y., LI H.Q., *A compact wide band filter based on the left handed material theory*, Microelectronic Engineering **85**(10), 2008: 2183-2186. https://doi.org/10.1016/j.mee.2008.07.014

[27] ABADLA M.M., TAYA S.A., *Excitation of TE surface polaritons on metal–NIM interfaces*, Optik **125**(3), 2014: 1401-1405. https://doi.org/10.1016/j.ijleo.2013.08.040

[28] TAYA S.A., EL-AMASSI D.M., *Reflection and transmission from left-handed material structures using Lorentz and Drude medium models*, Opto-Electronics Review **23**(3), 2015: 214-221. https://doi.org/10.1515/oere-2015-0031

[29] ABADLA M.M., TAYA S.A., *Theoretical investigation of guided modes in planar waveguides having chiral negative index metamaterial core layer*, Optik **131**, 2017: 562-573. https://doi.org/10.1016/j.ijleo.2016.11.184

[30] YOUNG K., KIM J., SOHN R., TAE H., *Guidance characteristics of circular metamaterial rod waveguide*, Asia-Pacific Microwave Conference, November 4-7, Seoul, Korea, Vol. 62, 2003: 203-215.

[31] SHADRIVOV I.V., *Nonlinear guided waves and symmetry breaking in left-handed waveguides*, Photonics and Nanostructures - Fundamentals and Applications **2**(3), 2004: 175-180. https://doi.org/10.1016/j.photonics.2004.08.003

[32] KULLAB H. M., TAYA S.A., EL-AGEZ T.M., *Metal-clad waveguide sensor using a left-handed material as a core layer*, Journal of the Optical Society of America B **29**(5), 2012: 959-964. https://doi.org/10.1364/JOSAB.29.000959

[33] KULLAB H.M., TAYA S.A., *Peak type metal-clad waveguide sensor using negative index materials*, AEU - International Journal of Electronics and Communications **67**(11), 2013: 984-986. https://doi.org/10.1016/j.aeue.2013.05.012

[34] KULLAB H.M., TAYA S.A., *Transverse magnetic peak type metal-clad optical waveguide sensor*, Optik **125**(1), 2014: 97-100. https://doi.org/10.1016/j.ijleo.2013.06.029

[35] TAYA S.A., KULLAB H.M., *Optimization of transverse electric peak-type metal-clad waveguide sensor using double-negative materials*, Applied Physics A **116**, 2014: 1841-1846. https://doi.org/10.1007/s00339-014-8338-y

[36] TAYA S.A., JARADA A.A., KULLAB H.M., *Slab waveguide sensor utilizing left-handed material core and substrate layers*, Optik **127**(19), 2016: 7732-7739. https://doi.org/10.1016/j.ijleo.2016.05.095

[37] TAYA S.A., MAHDI S.S., ALKANOO A.A., QADOURA I.M., *Slab waveguide with conducting interfaces as an efficient optical sensor: TE case*, Journal of Modern Optics **64**(8), 2017: 836-843. https://doi.org/10.1080/09500340.2016.1262072

[38] TAYA S.A., SHAHEEN S.A., ALKANOO A.A., *Photonic crystal as a refractometric sensor operated in reflection mode*, Superlattices and Microstructures **101**, 2017: 299-305. https://doi.org/10.1016/j.spmi.2016.11.057

[39] SUWAILAM M.M.B., CHEN Z.Z., *Surface waves on a grounded double-negative (DNG) slab waveguide*, Microwave and Optical Technology Letters **44**(6), 2005: 494-498. https://doi.org/10.1002/mop.20677

[40] KURSEEVA V., TIKHOV S., VALOVIK D., *Electromagnetic wave propagation in a layer with power nonlinearity*, Journal of Nonlinear Optical Physics & Materials **28**(1), 2019: 1950009. https://doi.org/10.1142/S0218863519500097

[41] EL-WASIFE K., SHABAT M., YASSIN S., *Nonlinear TE electromagnetic surface waves in a ferrite layered structure*, An-Najah University Journal for Research - A (Natural Sciences) **18**(2), 2004: 215-236.

Received May 28, 2023
in revised form October 2, 2023